

Continuum model of polygonization of carbon nanotubes

Dmitry Golovaty* and Shannon Talbott

Department of Theoretical and Applied Mathematics, The University of Akron, Akron, Ohio 44325-4002, USA

(Received 20 November 2007; published 13 February 2008)

We derive a simple continuum model of multiwalled carbon nanotubes that takes into account both strong covalent bonds within graphene layers and weak bonds between graphene layers. The model predicts polygonization of cross sections of large multiwalled nanotubes.

DOI: 10.1103/PhysRevB.77.081406

PACS number(s): 61.48.-c, 61.46.Fg, 61.50.Ah, 62.25.-g

I. INTRODUCTION

Polygonization of cross sections of large multiwalled carbon nanotubes (MWNTs), has been observed in a number of studies.¹⁻³ The physics of this phenomenon is generally well understood—the curvature-induced mismatch between the lattices of the adjacent graphene walls can be reduced by flattening the walls at the expense of creating the line defects that run parallel to the axis of the tube.³

Given that its mechanism is intuitively clear, it is surprising that polygonization of large MWNTs has not been theoretically confirmed by the standard modeling approaches. The reasons for this vary: the atomistic simulations of large tubes are too computationally expensive; the continuum models⁴⁻⁶ are based on energies that are invariant with respect to relative shifts and rotations of lattices within the walls. Even though semipolygonal cross sections of the bent MWNT were observed in continuum simulations⁶, they form by the Yoshimura mechanism⁷ unrelated to the lattice structure of the walls.

To our knowledge, the only existing model³ of polygonization of MWNTs relies on extending fitted small-systems energetics to large polygonized MWNTs. Then the feasibility of polygonization of MWNT is established by comparing the energies of various configurations. Besides the *ad hoc* energy approximation, the main drawback of this approach is that it does not consider other, noncircular and nonpolygonal configurations that may minimize the approximate expression for the energy. In a related work⁸, the energetics of collapse of carbon nanotubes as the diameter of tubes increases was explored using atomistic simulations.

In this paper we derive a continuum theory of MWNTs by upscaling a simple atomistic model that takes into account both strong covalent bonds between the atoms in a graphene layer and weak bonds between the atoms in adjacent layers. Even though the model is exceedingly simple, it shows that large MWNTs polygonize in order to minimize the Ginzburg-Landau-type energy. The turbostraticity of the tube is taken into account via a parameter equal to the difference between the number of atoms in the adjacent layers. The result is obtained without *a priori* restrictions on the shape of the tube and the appropriate form of the macroscopic energy.

The model confirms that polygonization of MWNTs occurs as the result of a competition between the interactions within individual graphene layers and the interactions between the layers and it is controlled by the diameter but not the number of walls in the MWNTs. We take advantage of the last observation by considering the simplest case of a two-walled carbon nanotube.

To simplify the mathematics even further, we assume that the walls of the nanotube are parallel so that the nanotube can be represented by a cross section perpendicular to the axis of the tube. Then the resulting system of the two concentric curves can be endowed with the atomic structure by “projecting” the atoms of the graphene walls onto the curves. For each curve, the distances between atoms depend on the chirality of the corresponding wall and may vary along the curve.

Further, we will assume that the diameter of each tube is much larger than the length of an interatomic bond in a hexagonal carbon lattice. Then a *microscale* object has dimensions of order of the carbon bond length and a *macroscale* object has dimensions of order of the diameter of the nanotube.

A. Macroscopic geometry

Suppose that two smooth, closed concentric curves \tilde{C}_1 and \tilde{C}_2 represent a cross section of a two-walled carbon nanotube by a plane perpendicular to the axis of the tube (Fig. 1). We will assume that these curves are parallel; that is, the distance between \tilde{C}_1 and \tilde{C}_2 when measured along any normal to \tilde{C}_1 is equal to the same constant value of d . The \mathbf{R}^2 -valued function $\tilde{\mathbf{r}}_1(\tilde{s})$ parametrizes \tilde{C}_1 with respect to its arclength $\tilde{s} \in [0, L]$ measured counterclockwise from some fixed initial point $\mathbf{r}(\tilde{0})$. Here L is the length of \tilde{C}_1 .

An orthogonal frame at $\tilde{\mathbf{r}}_1(\tilde{s})$ is given by a pair $(\mathbf{T}(\tilde{s}), \mathbf{N}(\tilde{s}))$ with $\mathbf{T}(\tilde{s}) = -\tilde{\mathbf{r}}_1'(\tilde{s}) = \langle \cos \theta(\tilde{s}), \sin \theta(\tilde{s}) \rangle$ and $\mathbf{N}(\tilde{s}) = \langle -\sin \theta(\tilde{s}), \cos \theta(\tilde{s}) \rangle$, where $\theta(\tilde{s})$ is the angle between $\mathbf{T}(\tilde{s})$ and the x axis at the point $\tilde{\mathbf{r}}_1(\tilde{s})$. The curvature of \tilde{C}_1 can be

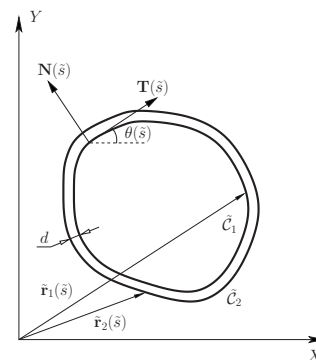
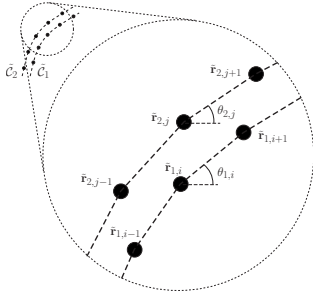


FIG. 1. Cross section of a two-walled carbon nanotube.

FIG. 2. Positions of atoms on curves C_1 and C_2 .

computed via the relation $\kappa(\tilde{s}) = \theta'(\tilde{s})$. Then, according to the Frenet formulas, $\mathbf{T}'(\tilde{s}) = \kappa(\tilde{s})\mathbf{N}(\tilde{s})$ and $\mathbf{N}'(\tilde{s}) = -\kappa(\tilde{s})\mathbf{T}(\tilde{s})$.

In what follows, we will require that $d\kappa(\tilde{s}) < 1$ for all $\tilde{s} \in [0, L]$. This assumption is physically reasonable as it automatically holds for any nanotube with a convex cross section, and it only rules out relatively large inward folds of the curve \tilde{C}_1 . Then we can parametrize \tilde{C}_2 with respect to \tilde{s} by setting $\tilde{\mathbf{r}}_2(\tilde{s}) = \tilde{\mathbf{r}}_1(\tilde{s}) + d\mathbf{N}(\tilde{s})$.

Note that \tilde{s} is not an arclength parameter for $\tilde{\mathbf{r}}_2$. Indeed, $\tilde{\mathbf{r}}_2'(\tilde{s}) = -[1 + d\kappa(\tilde{s})]\mathbf{T}(\tilde{s})$ and the distance traveled along \tilde{C}_2 from $\tilde{\mathbf{r}}_2(0)$ to $\tilde{\mathbf{r}}_2(\tilde{s})$ is $l(\tilde{s}) = \int_0^{\tilde{s}} [1 + d\kappa(\sigma)] d\sigma = \tilde{s} + [\theta(\tilde{s}) - \theta(0)]d$ while the distance traveled along \tilde{C}_1 from $\tilde{\mathbf{r}}_1(0)$ to $\tilde{\mathbf{r}}_1(\tilde{s})$ is equal to \tilde{s} . Then the running difference between the distances traveled along \tilde{C}_2 and \tilde{C}_1 is $\mathcal{L}(\tilde{s}) = l(\tilde{s}) - \tilde{s} = d[\theta(\tilde{s}) - \theta(0)]$ and the overall difference between the lengths of the two curves is $\mathcal{L}(L) = 2\pi d$. Further, by an appropriate rotation of coordinates, we can set $\theta(0) = 0$ to obtain

$$\mathcal{L}(\tilde{s}) = d\theta(\tilde{s}). \quad (1)$$

B. Microscopic structure

Since for mathematical simplicity we operate with cross sections of nanotubes that are intrinsically one dimensional (while the hexagonal atomic lattice of graphene is two dimensional), we will assume that the projection of the lattice on each cross section forms a one-dimensional chain of atoms. Although this assumption might not lead to a quantitatively accurate effective continuum model, we expect that the effective model based on physically reasonable assumptions should be qualitatively accurate.

Suppose that two sets (chains) of equidistant carbon atoms are embedded in the curves \tilde{C}_1 and \tilde{C}_2 , respectively, as shown in Fig. 2. The distance between the neighboring atoms in each chain will be set equal to the same constant h to reflect the fact that the atoms within a graphene layer are connected by essentially inextensible strong sp^2 σ bonds. Then the curve \tilde{C}_2 contains $n = \frac{2\pi d}{h}$ more atoms than the curve \tilde{C}_1 .

C. Energy

We will assume that the overall energy of the two-curve system consists of two parts: the energy due to bending of

the adjacent bonds and the energy due to weak delocalized π bonds between the atoms embedded in \tilde{C}_1 and \tilde{C}_2 , respectively.

Suppose that the energy associated with two bonds joined at an angle θ is $f(\theta)$ where $f: (0, 2\pi) \rightarrow \mathbf{R}$ is a smooth convex nondimensional function that has a minimum value of 0 at $\theta = \pi$ and satisfies the symmetry condition $f(\pi - \theta) = f(\pi + \theta)$. Further, let the weak interaction between the atoms in \tilde{C}_1 and \tilde{C}_2 be described by a Lennard-Jones-type potential $g(r) = (\frac{1}{r})^{12} - (\frac{1}{r})^6$. Then the total energy of the system is

$$\begin{aligned} \tilde{E} = & \tilde{\alpha} \sum_{i=1}^N f(\pi + \theta_{1,i} - \theta_{1,i+1}) + \tilde{\alpha} \sum_{j=1}^{N+n} f(\pi + \theta_{2,j} - \theta_{2,j+1}) \\ & + \tilde{\gamma} \sum_{i=1}^N \sum_{j=1}^{N+n} g\left(\frac{|\tilde{\mathbf{r}}_{1,i} - \tilde{\mathbf{r}}_{2,j}|}{d}\right), \end{aligned}$$

where $\tilde{\alpha}$ and $\tilde{\gamma}$ are the dimensional scaling factors, N is the number of atoms embedded in \tilde{C}_1 , $\theta_{1,N+1} = \theta_{1,1} + 2\pi$, and $\theta_{2,N+n+1} = \theta_{2,1} + 2\pi$.

From now on we will assume that $d, h \ll L$ and $n = \frac{2\pi d}{h} > 2$ is a fixed positive integer. Nondimensionalizing the variables $\mathbf{r} = \tilde{\mathbf{r}}/L$ and $s = \tilde{s}/L$ and rescaling \tilde{E} by $\tilde{\gamma}$, the non-dimensional energy is

$$\begin{aligned} E = & \alpha \sum_{i=1}^N f(\pi + \theta_{1,i} - \theta_{1,i+1}) + \alpha \sum_{j=1}^{N+n} f(\pi + \theta_{2,j} - \theta_{2,j+1}) \\ & + \sum_{i=1}^N \sum_{j=1}^{N+n} g\left(\frac{|\mathbf{r}_{1,i} - \mathbf{r}_{2,j}|}{\delta}\right), \end{aligned} \quad (2)$$

where $\delta = d/L \ll 1$, $\epsilon = h/L \ll 1$, and $\alpha = \tilde{\alpha}/\tilde{\gamma}$ are the nondimensional parameters of the system. Further, we will set C_1 and C_2 to represent \tilde{C}_1 and \tilde{C}_2 in nondimensional variables.

To justify the assumption that n can be held fixed in the minimization procedure, consider the experimental data¹ showing that the interwall spacing \hat{d}_{002} decreases from 0.39 to 0.34 as the diameter of the tube increases. The variation of interwall spacings for the entire range of nanotube diameters is of the order of $0.39 - 0.34 = 0.05$ nm—smaller than the carbon bond length of 0.142 nm. As a consequence, the integer part of the ratio of d/h remains the same for all diameters.

II. EFFECTIVE MODEL

Using the smoothness of \mathbf{r}_1 we have that $\theta_{1,i+1} - \theta_{1,i} = \theta'(s_i)\epsilon + o(\epsilon)$ for every $i = 1, \dots, N$, where s_i denotes the position of the i th atom on the curve C_1 . Since f is smooth, the symmetry of f and the fact that it has a minimum at $\theta = \pi$ imply that $f(\pi + \theta_{1,i} - \theta_{1,i+1}) = \frac{1}{2}f''(\pi)[\theta'(s_i)]^2\epsilon^2 + o(\epsilon^2)$ for every $i = 1, \dots, N$. Then

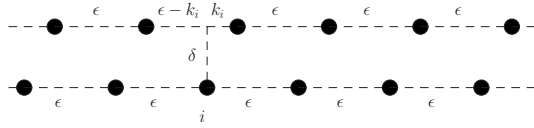


FIG. 3. Two offset chains of atoms.

$$\begin{aligned} \alpha \sum_{i=1}^N f(\pi + \theta_{1,i} - \theta_{1,i+1}) &= \alpha \epsilon \left[\sum_{i=1}^N \frac{1}{2} f''(\pi) [\theta'(s_i)]^2 \epsilon \right] + o(\epsilon) \\ &= \frac{\alpha \epsilon f''(\pi)}{2} \int_0^1 (\theta')^2 ds + o(\epsilon). \end{aligned} \quad (3)$$

Since exactly the same argument applies to the analogous sum over the curve \mathcal{C}_2 , we have that the leading contribution to the total energy due to bending of interatomic bonds is

$$E_b = \frac{\mu \epsilon}{2} \int_0^1 (\theta')^2 ds, \quad (4)$$

where $\mu = 2\alpha f''(\pi)$. This equation⁵ corresponds to the well-known Euler elastica model for long slender beams.⁹

Next we develop the effective expression for the weak interaction energy. Fix an atom i on an inner curve \mathcal{C}_1 and let $A = O(\epsilon^{1/2})$ be an arbitrary number that we can use as a ‘‘mesoscale’’ because $\epsilon \ll A \ll 1$. Set Λ_i^A to be the set of all atoms on the curve \mathcal{C}_2 that are closer than A to the atom i . Then $\sum_{j=1}^{N+n} g\left(\frac{|\mathbf{r}_{1,i} - \mathbf{r}_{2,j}|}{\delta}\right) = \sum_{j \in \Lambda_i^A} g\left(\frac{|\mathbf{r}_{1,i} - \mathbf{r}_{2,j}|}{\delta}\right) + \sum_{j \notin \Lambda_i^A} g\left(\frac{|\mathbf{r}_{1,i} - \mathbf{r}_{2,j}|}{\delta}\right)$. The second sum can be approximated as follows:

$$\sum_{j \notin \Lambda_i^A} g\left(\frac{|\mathbf{r}_{1,i} - \mathbf{r}_{2,j}|}{\delta}\right) \sim \left(\frac{\delta}{A}\right)^6 \frac{1}{\epsilon} = o(\epsilon^2), \quad (5)$$

because

$$\delta/\epsilon = d/h = n/2\pi. \quad (6)$$

Having estimated the contribution to the weak interaction energy from the atoms on \mathcal{C}_2 that are mesoscopically distant from the atom $i \in \mathcal{C}_1$, we now estimate the contribution to the energy due to the atoms that are mesoscopically close to the atom i . Since the curve \mathcal{C}_2 is smooth and since $A \ll 1$, the part of the curve \mathcal{C}_2 that is closer than A to the atom i can be approximated by the tangent line to \mathcal{C}_2 at the point s_i . That is, locally, we have a situation depicted in Fig. 3—in the macroscopically small neighborhood of the atom i the curves appear as two infinite straight lines of atoms offset by some distance k_i when viewed from the microscopic perspective. Therefore the energy of weak interaction between the atom i and the atoms in Λ_i^A is

$$\sum_{j \in \Lambda_i^A} g\left(\frac{|\mathbf{r}_{1,i} - \mathbf{r}_{2,j}|}{\delta}\right) \sim \sum_{j=-\infty}^{\infty} g\left(\frac{\sqrt{(\epsilon j + k_i)^2 + \delta^2}}{\delta}\right), \quad (7)$$

to the leading order in ϵ .

Note that, up to a term of order ϵ , the offset k_i between the two lattices at the point s_i is equal to the running difference $\mathcal{L}(s_i)$ between the two arclengths as measured from the points $\mathbf{r}_1(0)$ and $\mathbf{r}_2(0)$, respectively. Using Eqs. (1) and (6) we obtain that

$$\sum_{j=-\infty}^{\infty} g\left(\frac{\sqrt{(\epsilon j + k_i)^2 + \delta^2}}{\delta}\right) = G(\theta(s_i), n), \quad (8)$$

where

$$G(\theta, n) := \sum_{j=-\infty}^{\infty} g\left(\sqrt{\left(\frac{2\pi j}{n} + \theta\right)^2 + 1}\right). \quad (9)$$

Finally,

$$\begin{aligned} \sum_{i=1}^N \sum_{j=1}^{N+n} g\left(\frac{|\mathbf{r}_{1,i} - \mathbf{r}_{2,j}|}{\delta}\right) &= \sum_{i=1}^N G(\theta(s_i), n) + o(1) \\ &= \frac{1}{\epsilon} \int_0^1 G(\theta(s), n) ds + o(1) = E_w + o(1), \end{aligned} \quad (10)$$

and the leading contribution to the total effective energy is given by a Ginzburg-Landau-type expression

$$E_{eff} = E_b + E_w = \int_0^1 \left(\frac{\epsilon \mu}{2} (\theta')^2 + \frac{1}{\epsilon} G(\theta, n) \right) ds, \quad (11)$$

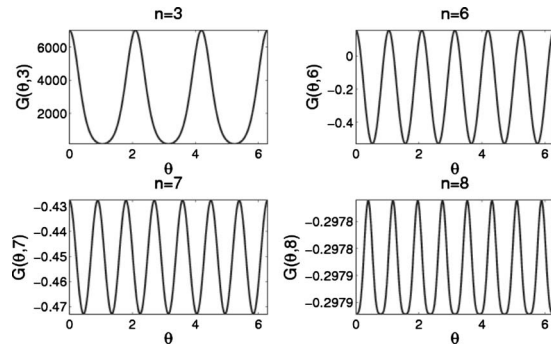
where ϵ can be viewed as an analog of the Ginzburg-Landau parameter.

Note that an expression similar to Eq. (8) can be easily developed if, for example, the interatomic distances for \mathcal{C}_1 and \mathcal{C}_2 are not the same and their ratio is equal to a small integer. Then one can introduce an analog of the offset k_i that is constant on the mesoscopic scale and hence can be interpreted as a macroscopic parameter. On the other hand, if the ratio of the interatomic distances is an irrational number that is not too close to 1, then k_i varies on the mesoscopic scale and the function G is constant. The effective energy in this case reduces to the elastica term which is minimized when the MWNT is circular. These scenarios describe MWNTs with walls of different chirality and are beyond the scope of the present paper.

We finish this section by discussing the properties of the function G . Although G is defined for all of θ and n , only integer values of n are physically relevant as n is equal to the difference between the number of atoms on the outer curve \mathcal{C}_2 and the inner curve \mathcal{C}_1 . Then, by construction, the function G is $2\pi/n$ periodic in θ and it has exactly n minima on the interval $[0, 2\pi]$. The profile of G for various values of n is shown in Fig 4.

III. NUMERICAL RESULTS AND DISCUSSION

To summarize, in our effective model a cross section of a two-walled nanotube is represented by a single curve $\mathcal{C} = \mathcal{C}_1$ with the effective energy given by Eq. (11). The equilibrium shape of the nanotube then minimizes the energy E_{eff} subject to the constraints

FIG. 4. $G(\theta, n)$ for the different values of n .

$$\int_0^1 \sin \theta ds = \int_0^1 \cos \theta ds = 0 \quad (12)$$

on the function θ that enforce the closedness of \mathcal{C} .

The values of the energy-minimizing function Θ will reside mostly at the minima of $G(\theta, n)$ due to the “penalty” term $\frac{1}{\epsilon}G(\theta, n)$. The function Θ transitions between two constant values over the narrow “interfacial” region; the width of this region decreases with ϵ . Because Θ increments by 2π as the curve \mathcal{C} is traversed in the counterclockwise direction and because G has n minima on the interval $[0, 2\pi]$, the minimizing configuration Θ should have exactly n interfaces separating n regions where Θ is almost constant. Note that n is equal to the number of “extra” atoms on the circumference of the outer tube and it is independent of the diameter of the inner tube (as long as the difference between the diameters of two tubes remains constant).

Since $\epsilon = h/L$, we have that $\epsilon \rightarrow 0$ when $L \rightarrow \infty$ and then the transition between the regions of constant θ must be sharper for the tubes with the larger radii. On the other hand, the interfacial regions smear out when L is small and the gradient term in the energy dominates. This effect has a clear physical explanation—the energy due to the curvature-induced mismatch between the lattices of the inner and the outer tubes increases with the diameter of the tube while the energy of a corner is independent of the diameter. The number of corners needed to remove the curvature and to introduce the equilibrium lattice stacking is equal to the difference between the number of atoms along circumferences of the outer and inner tubes. (Each corner “resets” the lattice to incorporate an extra atom into the outer tube.)

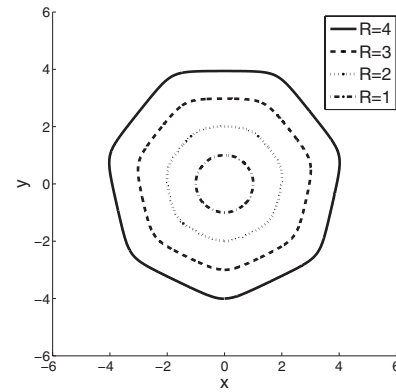


FIG. 5. Shape of a nanotube as a function of its diameter.

Observe that the interfaces in our “diffuse-type model” are not sharp—rather, the width of the interfacial regions increases continuously with ϵ . Consequently, the transition between the polygonal and the circular nanotube shapes is not sharp and the polygonal cross sections should continuously morph into the circular ones as the radius of the MWNT decreases. In other words, when the walls in a MWNT have the same chirality, circular cross sections are *never* energy minimizing and the shapes of smaller MWNTs are only close to being circular.

If we assume that the minimizer has the symmetry $\theta(\frac{1}{2}+s) = 2\pi - \theta(\frac{1}{2}-s)$, then the constraints (12) are automatically satisfied and the minimizer solves the boundary value problem

$$\epsilon^2 \mu \theta'' - G_\theta(\theta, n) = 0, \quad 0 < s < \frac{1}{2},$$

$$\theta(0) = 0, \quad \theta\left(\frac{1}{2}\right) = \pi. \quad (13)$$

This problem was solved numerically using the MATLAB BVP solver¹⁰ assuming that \mathcal{C}_2 contains seven more atoms than \mathcal{C}_1 . The shapes of nanotubes of different circumferences are shown in Fig. 5 and correspond to the trends observed experimentally.¹

ACKNOWLEDGMENTS

The authors thank A. Buldum for bringing our attention to the problem and Pat Wilber for many useful discussions. This work was supported by NSF Grant No. DMS 0407361.

*dmitry@math.uakron.edu

¹C.-H. Kiang, M. Endo, P. M. Ajayan, G. Dresselhaus, and M. S. Dresselhaus, *Phys. Rev. Lett.* **81**, 1869 (1998).

²F. Y. Wu and H. M. Cheng, *J. Phys. D* **38**, 4302 (2005).

³M. Yoon, J. Howe, G. Tibbetts, G. Eres, and Z. Zhang, *Phys. Rev. B* **75**, 165402 (2007).

⁴B. I. Yakobson, C. J. Brabec, and J. Bernholc, *Phys. Rev. Lett.* **76**, 2511 (1996).

⁵M. Arroyo and T. Belytschko, *Phys. Rev. B* **69**, 115415 (2004).

⁶M. Arroyo and T. Belytschko, *Int. J. Numer. Methods Eng.* **59**,

419 (2004).

⁷Z. Bažant and L. Cedolin, *Stability of Structures* (Oxford University Press, New York, 1991).

⁸S. Zhang, R. Khare, T. Belytschko, K. J. Hsia, S. L. Mielke, and G. C. Schatz, *Phys. Rev. B* **73**, 075423 (2006).

⁹S. S. Antman, *Nonlinear Problems of Elasticity*, 2nd ed., Vol. 107 of Applied Mathematical Sciences (Springer, New York, 2005).

¹⁰MATLAB is a registered trademark of The MathWorks, Inc. <http://www.mathworks.com>